Inorg. Chem. **2008**, *47*, 4891−4902

Coordination Asymmetry in Divanadium(V) Compounds Containing a V_2O_3 Core: Synthesis, Characterization, and Redox Properties

Pabitra Baran Chatterjee,[†] Subhajit Bhattacharya,[†] Anandalok Audhya,[†] Ki-Young Choi,[‡] Akira Endo,[§] and Muktimoy Chaudhury*,[†]

Department of Inorganic Chemistry, Indian Association for the Cultivation of Science, Kolkata 700 032, India, Department of Chemistry Education, Kongju National University, Kongju 314-701, South Korea, and Department of Chemistry, Faculty of Science and Technology, Sophia University, 7-1, Kioi-cho, Chiyoda-ku, Tokyo 102-8554, Japan

Received February 2, 2008

A general protocol for the synthesis of μ-oxo divanadium(V) compounds [LOV(μ-O)VO(Salen)] (**1**−**5**) incorporating coordination asymmetry has been developed for the first time. One of the vanadium centers in these compounds has an octahedral environment, completed by tetradentate Salen ligand, while the remaining center has square pyramidal geometry, made up of tridentate biprotic Schiff-base ligands (L^{2-}) with ONO (**1**−**3**) and ONS (**4**, **5**) type donor combinations. Single crystal X-ray diffraction analysis, ESI-MS, and NMR (both ^{1}H and ^{51}V) spectroscopy have been used extensively to establish their identities. The V(1)−O(6)−V(2) bridge angle in these compounds, save **3**, lie in a narrow range (166.20(9)−157.79(16)°) with the V_2O_3 core having a rare type of *twist*-angular structure, somewhat intermediate between the regular *anti*-linear and the *syn*-angular modes. For **3**, however, the bridge angle is sufficiently smaller 117.92(8)° that it forces the V_2O_3 core to adopt an *anti*-angular geometry. The V(1)···V(2) separations in these molecules (3.7921(7)−3.3084(6) Å) are by far the largest compared to their peers containing a V_2O_3 core. The molecules retain the binuclear structures also in solution as confirmed by NMR spectroscopy. Their redox behaviors appear quite interesting, each undergoing a one-electron reduction in the positive potential range ($E_{1/2}$, 0.42−0.45 V vs Ag/AgCl) to generate a trapped-valence mixed-oxidation products $[LV^{V}O\text{-}(\mu\text{-}O)\text{-}OV^{IV}(salen)]^{1-}$, confirmed by combined coulometry-EPR experiments. The bent V−O−V bridge in these molecules probably prevents the symmetry-constrained vanadium d_{xy} orbitals, containing the unpaired electron, to overlap effectively via the pπ orbitals of the bridging oxygen atom, thus accounting for the trapped-valence situation in this case.

Introduction

The lack of symmetry in the coordination environment of binuclear active sites of many metalloenzymes is an important structural feature that plays the decisive role in the mechanisms of substrate turnover.[1] Ligands providing donor set and coordination number asymmetry in tandem thus contribute effectively in the synthesis of biomimetic model compounds to replicate metallobiosites.[2] Moreover, such unsymmetrical bimetallic compounds have also attracted considerable interest, mainly because of their catalytic properties. Several methodologies have been adopted in the literature to synthesize unsymmetrical binuclear compounds. A few such approaches[3] involve targeted synthesis of single

* To whom correspondence should be addressed. E-mail: icmc@iacs.res.in.
† Indian Association for the Cultivation of Science.
‡ Kongju National University.
§ Sophia University.

(1) (a) Que, L., Jr.; True, A. E. *Prog. Inorg. Chem.* **1990**, *38*, 97. (b) Vincent, J. B.; Olivier-Lilley, G. L.; Averill, B. A. *Chem. Rev.* **1990**, *90*, 1447. (c) Feig, A. L.; Lippard, S. J. *Chem. Rev.* **1994**, *94*, 759. (d) Magnus, K. A.; Hoa, T. T.; Carpenter, J. E. *Chem. Rev.* **1994**, *94*, 727.

(2) Satcher, J. H., Jr.; Droege, M. W.; Weakley, T. J. R.; Taylor, R. T. *Inorg. Chem.* **1995**, *34*, 3317.

(3) (a) Chufán, E. E.; Verani, C. N.; Puiu, S. C.; Rentschler, E.; Schatzschneider, U.; Incarvito, C.; Rheingold, A. L.; Karlin, K. D. *Inorg. Chem.* **2007**, *46*, 3017; and references therein. (b) Lee, S. C.; Holm, R. H. *J. Am. Chem. Soc.* **1993**, *115*, 11789; and references therein. (c) Nanthakumar, A.; Fox, S.; Murthy, N. N.; Karlin, K. D. *J. Am. Chem. Soc.* **1993**, *115*, 8513. (d) Kurtz, D. M., Jr. *Chem. Rev.* **1990**, *90*, 585; and references therein. (e) Singh, S.; Roesky, H. W. *J. Chem. Soc., Dalton Trans.* **2007**, 1360. (f) Liston, D. J.; Kennedy, B. J.; Murray, K. S.; West, B. O. *Inorg. Chem.* **1985**, *24*, 1561. (g) Yang, C.-H.; Goedken, V. L. *Inorg. Chim. Acta* **1986**, *117*, L19.

10.1021/ic800208w CCC: $40.75
Published on Web 05/02/2008

oxo-bridged bimetallic (both homo- and hetero-) compounds. Unfortunately, none of these protocols seems to work well for the synthesis of μ-oxo divanadium compounds. Nevertheless, in the literature at least thirty structurally characterized μ-oxo divanadium compounds containing a $V_2O_3^{n+}$ core ($n = 4$, 3, and 2) have been reported. All these compounds have symmetrical structures involving identical ligand molecule(s) attached to both the metal centers.[4–9] When the vanadium centers have octahedral geometry,[4–6] the majority of these compounds[5,6] have a linear V−O−V bridge with the terminal oxo-groups in mutually *trans* positions (*anti*-linear structure).[7b] On the other hand, when the vanadium centers have square pyramidal geometry,[7–9] the bridging and terminal oxygen atoms have a diverse range of arrangements, from *anti*-linear[8k,l] to *syn*-angular[7,8a,b] through *anti*-angular[8c–j] and *twist*-angular[9] structures.

We recently have reported the development of a synthetic protocol that led us to the isolation of μ-oxo divanadium(V) compounds with a hitherto unknown unsymmetrical combination involving an octahedral and a square pyramidal vanadium(V) center connected together by a single μ-oxo bridge.[10] To achieve this objective, we have used a tetradentate ligand, that is, *N*, *N*′-bis(salicylidene)-1,2-diaminoethane (H_2Salen) to generate the octahedral vanadium site while for the square pyramidal metal centers, tridentate biprotic dithiocarbazate based ligands (H_2L^4 and H_2L^5) have been employed. Herein, we have successfully applied the same preparative method on other tridentate biprotic ligands ($LiHL^1$−$LiHL^3$) to test the efficacy of this protocol as a general method for the preparation of unsymmetrical divanadium(V) compounds with a V_2O_3 core. The compounds [LOV(μ-O)VO(Salen)] (L = L^1−L^5; **1**−**5**) have been characterized by single crystal X-ray diffraction analysis, NMR (both ^{1}H and ^{51}V) and ESI-mass spectral studies. Redox properties of the compounds have been explored in detail.

Experimental Section

Materials. Unless stated otherwise, all reactions were carried out under an atmosphere of purified dinitrogen. The tridentate ligands [$LiHL^1$−$LiHL^3$, H_2L^4 and H_2L^5][11] and the precursor complexes [VO(acac)$_2$],[12] [VO(Salen)],[13] and [VOL(H$_2$O)][14] (L = L^1−L^3) were prepared following the reported methods. All other reagents are commercially available and used as received. Solvents were reagent grade, dried by standard methods,[15] and distilled under nitrogen prior to their use.

Preparation of Complexes. [L^1OV(μ-O)VO(Salen)] (1). About 0.17 g (0.5 mmol) of [VO(Salen)] was dissolved in acetonitrile (30 mL). [VOL^1(H$_2$O)] (0.13 g, 0.5 mmol) in methanol (15 mL) was added to this solution. The resulting mixture was refluxed for about 3 h, when a green solution was obtained. It was cooled, filtered, and reduced to about a 20 mL volume by rotary evaporation. The solution was kept in the air for about 2 days, becoming gradually brown in color. Finally, it was cooled at 4 °C in a refrigerator for an overnight period. A brown crystalline compound deposited at this stage was collected by filtration, washed with diethyl ether (3 × 10 mL), and finally, dried in vacuo over P_4O_{10}. Yield: 0.2 g (70%). Anal. Calcd for $C_{25}H_{21}N_3O_8V_2$: C, 50.61; H, 3.57; N, 7.08. Found: C, 50.82; H, 3.41; N, 7.15%. FT-IR bands (KBr pellet, cm^{-1}): 1688s, 1624s, 1597s, 1550s, 1471m, 1448s, 1339m, 1275s, 953s, 912s, 883s, 817s, 759s, 660s, 460s. UV−vis (DMSO) [λ_{max}, nm (ε, mol^{-1} cm^2)]: 574 (614); 357 (11 900). ^{51}V NMR (500 MHz, DMSO-d_6, 299 K, δ/ppm): −533 (s, V(2)); −574 (s, V(1)). ESI-MS (positive) in CH_3CN: *m*/*z*, 595.04 [M + H$^+$].

[L^2OV(μ-O)VO(Salen)] (2). This compound was obtained as a brown crystalline solid following essentially the same procedure as described above for **1** using [VOL^2(H$_2$O)] and [VO(Salen)] as the precursor complexes in an acetonitrile/methanol solvent mixture (4:1 v/v, 30 mL). Yield: 57%. Anal. Calcd for $C_{25}H_{20}BrN_3O_8V_2$: C, 44.67; H, 3.00; N, 6.25. Found: C, 44.97; H, 2.82; N, 6.34%. FT-IR bands (KBr pellet, cm^{-1}): 1678s, 1620s, 1595s, 1553s, 1531m, 1459s, 1448m, 1340m, 1274s, 948s, 912s, 885s, 819s, 760s, 657s, 459s. UV−vis (DMSO) [λ_{max}, nm (ε, mol^{-1} cm^2)]: 575 (290); 362 (10 000); 260 (44 600). ^{51}V NMR (500 MHz, DMSO-d_6, 299 K, δ/ppm): −533 (s, V(2)); −574 (s, V(1)). ESI-MS (positive) in CH_3CN: *m*/*z*, 673.01 [M + H$^+$].

[L^3OV(μ-O)VO(Salen)]·H$_2$O (3). This compound was obtained in 38% yield following an identical procedure as described above for **1** using [VOL^3(H$_2$O)] and [VO(Salen)] as the precursor

(4) (a) Nishizawa, M.; Hirotsu, K.; Ooi, S.; Saito, K. *J. Chem. Soc., Chem. Commun.* **1979**, 707. (b) Kojima, A.; Okazaki, K.; Ooi, S.; Saito, K. *Inorg. Chem.* **1983**, *22*, 1168. (c) Schulz, D.; Weyhermüller, T.; Wieghardt, K.; Nuber, B. *Inorg. Chim. Acta* **1995**, *240*, 217. (d) Yamada, S.; Katayama, C.; Tanaka, J.; Tanaka, M. *Inorg. Chem.* **1984**, *23*, 253. (e) Hayton, T. W.; Patrick, B. O.; Legzdins, P. *Inorg. Chem.* **2004**, *43*, 7227. (f) Nielsen, K.; Rasmus, R.; Eriksen, K. M. *Inorg. Chem.* **1993**, *32*, 4825.

(5) (a) Launay, J.-P.; Jeannin, Y.; Daoudi, M. *Inorg. Chem.* **1985**, *24*, 1052. (b) Holwerda, R. A.; Whittlesey, B. R.; Nilges, M. *Inorg. Chem.* **1998**, *37*, 64. (c) Ghosh, S.; Nanda, K. K.; Addison, A. W.; Butcher, R. J. *Inorg. Chem.* **2002**, *41*, 2243. (d) Mahroof-Tahir, M.; Keramidas, A. D.; Goldfarb, R. B.; Anderson, O. P.; Miller, M. M.; Crans, D. C. *Inorg. Chem.* **1997**, *36*, 1657. (e) Toftlund, H.; Larsen, S.; Murray, K. S. *Inorg. Chem.* **1991**, *30*, 3964.

(6) (a) Knopp, P.; Wieghardt, K.; Nuber, B.; Weiss, J.; Sheldrick, W. S. *Inorg. Chem.* **1990**, *29*, 363. (b) Gruning, C.; Schmidt, H.; Rehder, D. *Inorg. Chem. Commun.* **1999**, *2*, 57.

(7) (a) Dutta, S. K.; Kumar, S. B.; Bhattacharyya, S.; Tiekink, E. R. T.; Chaudhury, M. *Inorg. Chem.* **1997**, *36*, 4954. (b) Dutta, S. K.; Samanta, S.; Kumar, S. B.; Han, O. H.; Burckel, P.; Pinkerton, A. A.; Chaudhury, M. *Inorg. Chem.* **1999**, *38*, 1982.

(8) (a) Pessoa, J. C.; Silva, J. A. L.; Vieira, A. L.; Vilas-Boas, L.; O′Brien, P.; Thornton, P. *J. Chem. Soc., Dalton Trans.* **1992**, 1745. (b) Hartung, J.; Dress, S.; Greb, M.; Schmidt, P.; Svoboda, I.; Fuess, H.; Murso, A.; Stalke, D. *Eur. J. Org. Chem.* **2003**, 2388. (c) Dutta, S.; Basu, P.; Chakravorty, A. *Inorg. Chem.* **1993**, *32*, 5343. (d) Ludwig, E.; Schilde, U.; Uhlemann, E.; Weller, F.; Dehnicke, K. *Z. Anorg. Allg. Chem.* **1993**, *619*, 669. (e) Sundheim, A.; Mattes, R. *Z. Naturforsch., B: Chem. Sci.* **1993**, *48*, 1848. (f) Chakravarty, J.; Dutta, S.; Chakravorty, A. *J. Chem. Soc., Dalton Trans.* **1993**, 2857. (g) Ludwig, E.; Hefele, H.; Schilde, U.; Uhlemann, E. *Z. Anorg. Allg. Chem.* **1994**, *620*, 346. (h) Dai, J.; Akiyama, S.; Munakata, M.; Mikuriya, M. *Polyhedron* **1994**, *13*, 2495. (i) Bellemin-Laponnaz, S.; Coleman, K. S.; Dierkes, P.; Masson, J. -P.; Osborn, J. A. *Eur. J. Inorg. Chem.* **2000**, 1645. (j) Dinda, R.; Sengupta, P.; Ghosh, S.; Mak, T. C. W. *Inorg. Chem.* **2002**, *41*, 1684. (k) Wang, D.; Behrens, A.; Farahbakhsh, M.; Gatjens, J.; Rehder, D. *Chem. Eur. J.* **2003**, *9*, 1805. (l) Pessoa, J. C.; Calhorda, M. J.; Cavaco, I.; Correio, I.; Duarte, M. T.; Felix, V.; Henriques, R. T.; Piedade, M. F. M.; Tomaz, I. *J. Chem. Soc., Dalton Trans.* **2002**, 4407.

(9) Mandal, S.; Ghosh, P.; Chakravorty, A. *Inorg. Chem.* **1997**, *36*, 59.

(10) A part of this work has been published as a rapid communication: Chatterjee, P. B.; Kundu, N.; Bhattacharya, S.; Choi, K.-Y.; Endo, A.; Chaudhury, M. *Inorg. Chem.* **2007**, *46*, 5483.

(11) (a) Ceccato, A. S.; Neves, A.; deBrito, M. A.; Drechset, S. M.; Mangrich, A. S.; Werner, R.; Haase, W.; Bortoluzzi, A. J. *J. Chem. Soc., Dalton Trans.* **2000**, 1573. (b) Ali, M. A.; Livingstone, S. C.; Philips, D. J. *Inorg. Chim. Acta* **1973**, *7*, 179.

(12) Rowe, R. A.; Jones, M. M. *Inorg. Synth.* **1957**, *5*, 113.

(13) Bonadies, J. A.; Carrano, C. J. *J. Am. Chem. Soc.* **1986**, *108*, 4088.

(14) Theroit, L. J.; Carlisle, G. O.; Hu, H. J. *J. Inorg. Nucl. Chem.* **1969**, *31*, 2841.

(15) Perrin, D. D.; Armarego, W. L. F.; Perrin, D. R. *Purification of Laboratory Chemicals*, 2nd ed.;Pergamon: Oxford, U.K., 1980.

Table 1. Summary of X-ray Crystallographic Data for the Complexes **2**, **3**, **4**, and **5**

parameter	**2**	**3**	**4**	**5**
composition	$C_{25}H_{20}BrN_3O_8V_2$	$C_{25}H_{22}N_4O_{11}V_2$	$C_{25}H_{22}N_4O_6S_2V_2$	$C_{27}H_{24}BrN_5O_6S_2V_2$
formula wt.	672.23	656.35	640.47	760.42
crystal system	triclinic	monoclinic	triclinic	triclinic
space group	$P\bar{1}$	$P2_1/c$	$P\bar{1}$	$P\bar{1}$
a, Å	10.1977(4)	14.3475(8)	9.9337(8)	11.1599(6)
b, Å	10.7622(5)	12.5778(7)	10.6502(9)	11.5448(7)
c, Å	12.2746(5)	14.9525(8)	13.4951(11)	14.1841(8)
α, deg	98.5640(10)	90.0000	107.3840(10)	81.3900(10)
β, deg	106.7520(10)	106.6890(10)	101.890(2)	67.0010(10)
γ, deg	96.4370(10)	90.0000	97.5190(10)	63.1810(10)
V, Å^3	1258.37(9)	2584.7(2)	1304.67(19)	1500.47(15)
D_{calc}, Mg m^{-3}	1.774	1.687	1.630	1.683
temp, K	293(2)	293(2)	293(2)	293(2)
λ (Mo Kα), Å	0.71073	0.71073	0.71073	0.71073
Z	2	4	2	2
F(000)	672	1336	652	764
$2\theta_{max}$ [°]	56.68	56.62	56.72	56.62
μ mm^{-1}	2.387	0.795	0.926	2.144
reflections collected/ unique	17469/6250	26269/6413	17705/6457	20677/7426
R_{int}/GOF on F^2	0.0239/1.009	0.0354/1.022	0.0290/1.052	0.0526/1.005
Data/ restraints/parameters	6250/0/352	6413/0/385	6457/0/352	7426/0/392
$R1(F_0)$, $wR2(F_0)$ ($I \geq 2\sigma(I)$)	0.0293, 0.0736	0.0368, 0.0842	0.0358, 0.0843	0.0466, 0.1020
$R1(F_0^2)$, $wR2(F_0^2)$ (all data)	0.0445, 0.0813	0.0579, 0.0979	0.0607, 0.0983	0.1104, 0.1314

complexes. Anal. Calcd for $C_{25}H_{22}N_4O_{11}V_2$: C, 45.75; H, 3.38; N, 8.54. Found: C, 45.52; H, 3.55; N, 8.41%. FT-IR bands (KBr pellet, cm^{-1}): 1660s, 1618s, 1598s, 1558s, 1497s, 1468m, 1443m, 1332s, 1270s, 964s, 903m, 822s, 767s, 658s, 461s. UV−vis (DMSO) [λ_{max}, nm (ε, mol^{-1} cm^2)]: 574 (600); 361 (26 500); 355 (27 400); 263 (41 000). ^{51}V NMR (500 MHz, DMSO-d_6, 299 K, δ/ppm): −531 (s, V(2)); −574 (s, V(1)). ESI-MS (positive) in CH_3CN: m/z, 639.99 [M − H_2O + H^+].

[L^4OV(μ-O)VO(Salen)] (4). To a stirred acetonitrile solution (10 mL) of [VO(acac)$_2$] (0.14 g, 0.5 mmol) was added an equimolar amount of the ligand H_2L^4 (0.11 g), taken in the same solvent (10 mL). The mixture was refluxed for 15 min to get a clear brown solution. To this was then added an acetonitrile solution (15 mL) of [VO(Salen)] (0.17 g, 0.5 mmol), and the resulting mixture was further refluxed for an additional period of 3 h to get a green solution. It was then filtered, the filtrate volume was reduced to about 20 mL using a rotary evaporator and allowed to stand in the air for about two days to become gradually brown in color. The solution was finally cooled at 4 °C in a refrigerator for an overnight period. A brown crystalline compound deposited at this stage was collected by filtration, washed with diethyl ether (3 × 10 mL), and dried in vacuo over P_4O_{10}. Yield: 0.13 g (40%). Anal. Calcd for $C_{25}H_{22}N_4O_6S_2V_2$: C, 46.88; H, 3.46; N, 8.75; S, 10.01. Found: C, 46.59; H, 3.38; N, 8.77; S, 9.96%. FT-IR bands (KBr pellet, cm^{-1}): 1620s, 1603s, 1556s, 1532s, 1475m, 1439m, 1273s, 953s, 917s, 853s, 816m, 763s, 655s, 456s. UV−vis (DMSO) [λ_{max}, nm (ε, mol^{-1} cm^2)]: 576 (2000); 353 (29 100); 346 (29 400); 302 (43 300). ^{51}V NMR (500 MHz, DMSO-d_6, 299 K, δ/ppm): −467 (s, V(2)); −574 (s, V(1)). ESI-MS (positive) in CH_3CN: m/z, 640.82 [M + H^+].

[L^5OV(μ-O)VO(Salen)]·CH_3CN (5). This compound was prepared as a brown crystalline solid following essentially the same procedure as described for **4** using H_2L^5 as the tridentate ligand. Yield: 48%. Anal. Calcd for $C_{27}H_{24}BrN_5O_6S_2V_2$: C, 42.65; H, 3.18; N, 9.21; S, 8.43. Found: C, 42.37; H, 3.19; N, 9.10; S, 8.39%. FT-IR bands (KBr pellet, cm^{-1}): 1624s, 1596s, 1556s, 1531s, 1458s, 1443s, 1273s, 1045m, 964s, 911s, 855s, 820s, 754s, 661s, 458s. UV−vis (DMSO) [λ_{max}, nm (ε, mol^{-1} cm^2)]: 578 (770); 353 (17 800); 289 (36 700); 277 (41 700). ^{51}V NMR (500 MHz, DMSO-d_6, 299 K, δ/ppm): −466 (s, V(2)); −574 (s, V(1)).

Physical Measurements. Elemental (C, H, N, and S) analyses were performed at IACS on a Perkin-Elmer model 2400 Series II CHNS Analyzer. UV−vis, IR, ESI-MS, ^{1}H and ^{51}V NMR spectra were recorded using the same instrumentation facilities as described elsewhere.[16]

Cyclic voltammetry (CV) in DMSO was recorded on a BAS model 100 B/W electrochemical workstation using a platinum disk (i.d. = 1.6 mm) working and a platinum wire counter electrode. Ag/AgCl was used for reference and Fc/Fc$^+$ couple as the internal standard.[17] Solutions were ∼1.0 mM in samples and contained 0.1 M TBAP as supporting electrolyte. Bulk electrolyses were carried out using a platinum-gauze working electrode at 298 K.

EPR spectra in DMSO solution (taken in a flat cell) were recorded on a JEOL Model JES-FA 300 X-band Spectrometer, equipped with a standard low temperature apparatus (at 77 K) and data processing system ESPRIT 330.

X-ray Crystallography. Diffraction quality crystals of **2** (block, brown crystals, 0.147 × 0.106 × 0.106 mm^3 obtained from acetonitrile/methanol (4:1 v/v) mixture), **3** (plate, black crystals, 0.321 × 0.232 × 0.101 mm^3 obtained from acetonitrile/methanol (4:1 v/v) mixture), **4** (block, black crystals, 0.308 × 0.213 × 0.192 mm^3 obtained from acetonitrile solution), and **5** (plate, black crystals, 0.28 × 0.149 × 0.063 mm^3 obtained from acetonitrile solution), were obtained from the designated solvents by slow evaporation at 4 °C. Intensity data for the compounds **2**−**5** were measured employing a Bruker SMART 1000 CCD diffractometer equipped with a monochromatized Mo Kα radiation (λ = 0.71073 Å) source using the $\omega/2\theta$ scan technique at 293(2) K. No crystal decay was observed during the data collection. Unfortunately, the crystals of **1** lose its solvent before data collection. Accurate cell parameters and orientation matrices were determined from setting angles of 5392, 3219, 6287, and 6804 reflections in the ranges 2.2915° ≤ θ ≤ 28.103°, 2.155° ≤ θ ≤ 27.608°, 2.3345° ≤ θ ≤ 28.3195°, and 2.180° ≤ θ ≤ 22.9555°, for **2**, **3**, **4**, and **5**,

(16) Chatterjee, P. B.; Mandal, D.; Audhya, A.; Choi, K.-Y.; Endo, A.; Chaudhury, M. *Inorg. Chem.* **2008**, 47; in press (MS ID: ic-2007−02286h)

(17) Gagné, R. R.; Koval, C. A.; Lisensky, G. C. *Inorg. Chem.* **1980**, *19*, 3854.

(18) Sheldrick, G. M. *SADABS, Program for Empirical Absorption Correction of Area Detector Data*; University of Göttingen: Göttingen, Germany, 1996.

respectively. The intensity data were corrected for empirical absorption. In all cases, absorption corrections based on multiscan using the *SADABS* software[18]were applied.

The structures were solved by direct methods[19] and refined on F^2 by a full-matrix least-squares procedure[19] with anisotropic displacement parameters for all the non-hydrogen atoms (except for the N(5) atom in **5**) based on all data minimizing $wR = [\Sigma\,[w((F_0^2 - F_c^2)^2]/\Sigma\, w\,(F_0^2)^2]^{1/2}$, $R = \Sigma||F_0| - |F_c||/\Sigma|F_0|$, and $S = [\Sigma[w(F_0^2 - F_c^2)^2]/(n - p)]^{1/2}$. SHELXL-97 was used for both structure solutions and structure refinements.[20] The centric distribution of intensities indicated the space group $P\bar{1}$ for **2**, **4**, and **5**, and the systematic absences indicated the space group to be $P2_1/c$ for **3**. A summary of the relevant crystallographic data and the final refinement details are given in Table 1. The hydrogen atoms except on the solvent of crystallization (in the case of **3**) and H(10) and H(23) (in **5**) were calculated and isotropically fixed in the final refinement [d(C−H) = 0.95 Å, with the isotropic thermal parameter of U_{iso}(H) = 1.2 U_{iso}(C)]. In **3**, the nonligated oxygen bound hydrogen atoms and, in **5**, the C(10) and C(23) bound hydrogen atoms have been located directly from Fourier difference maps and refined isotropically with 100% site occupancy factors each. In **5**, also the N(5) atom was refined isotropically. The SMART and SAINT-plus software packages[21] were used for data collection and reduction, respectively. Crystallographic diagrams were drawn using the ORTEP-3 software package[22] at 30% probability level.

Results and Discussion

Syntheses. Unsupported oxo-bridged divanadium(V) compounds [LOV(μ-O)VO(Salen)] (**1**−**5**) involving a pair of dissimilar ligands, providing coordination asymmetry, have been prepared for the first time through a single-pot synthesis. The strategy adopted for such synthesis is displayed in Scheme 1. All the product molecules contain a $[V_2O_3]^{4+}$ core involving a μ-oxo bridge, flanked by an octahedral and a square pyramidal vanadium(V) center. To achieve this goal, we have chosen [VO(Salen)] as the precursor compound to generate the octahedral vanadium site. This compound is known to get aerially oxidized to $[VO(Salen)]^+$ in the presence of added anions, that is, ClO_4^-, BF_4^-, and so forth.[23] The vanadium centers in these oxidized compounds have octahedral geometry with the incoming anions being accommodated into the vacant coordination site of the metal ion, *trans* to the terminal oxo- group. For the generation of the square pyramidal vanadium(V) center, tridentate biprotic Schiff-base ligands LiHL (L = L^1−L^3) and H_2L (L = L^4 and L^5) have been chosen. The dithiocarbazate-based ligands H_2L^4 and H_2L^5 can produce square pyramidal *cis*-dioxo anionic species $[LV^VO_2]^-$ when the ligands are refluxed with $[VO(acac)_2]$ in acetonitrile in the presence of an added cation.[24] In the actual protocol (as outlined in Scheme 1), stoichiometric amounts of $[VOL(H_2O)]$ (L = L^1−L^3) and $[V^{IV}O(Salen)]$ (1:1 mol ratio) have been taken in acetonitrile-methanol (2:1 v/v) solvent mixture while for the rest of the compounds, $[V^{IV}O(acac)_2]$, H_2L (L = L^4 and L^5) and $[V^{IV}O(Salen)]$ (in 1:1:1 mol ratio) are combined in neat acetonitrile. The resulting solutions have been refluxed and subsequently exposed to the atmospheric oxygen to get both $[V^VO(Salen)]^+$ and $[LV^VO_2]^-$ species together, thus allowing the anionic species to be accommodated into the vacant coordination site of $[VO(Salen)]^+$, leading to the desired products **1**−**5** as brown crystalline solids in moderate to high yields (45−70%). The formation of $[V^VO(Salen)]^+$, we anticipate, is favored by the anion ($[LV^VO_2]^-$) assisted oxidation of $[V^{IV}O(Salen)]$,[23] while that of $[LV^VO_2]^-$ is facilitated by the cation ($[V^VO(Salen)]^+$) assisted oxidation of the putative species $[LV^{IV}O(solvent)]$.[24] The products (**1**−**5**) obtained are appreciably soluble only in DMSO.

The IR spectra of the complexes (**1**−**5**) are summarized in the Experimental Section, containing all the pertinent bands of the coordinated pair of ligands. These include a couple of strong bands at about 1620 and 1600 cm^{-1} regions due to the υ(C═N) stretching modes of the coordinated Schiff base moieties.[7,9,24,25] The carboxylate part of the complexes **1**−**3** also displays a pair of strong bands at about 1690−1660 and 1350−1330 cm^{-1} regions corresponding to υ_{asym}(COO) and υ_{sym}(COO) vibrations, respectively, as expected for an unidentate carboxylato group with characteristically large $\Delta\upsilon$ separation (ca. 350 cm^{-1}).[26] A prominent band at 1270−1275 cm^{-1} due to υ(C−O/phenolate) also appears in all these complexes. In addition, a couple of strong bands appearing in the 903−916 and 948−964 cm^{-1} regions provide a signature for the terminal V═O_t stretching, corresponding to the individual vanadium centers of the binuclear compounds. The μ-oxo bridge which connects the vanadium centers together provides a moderately strong antisymmetric bridge vibrations in the region 816−822 cm^{-1}.[7]

Mass Spectroscopy. ESI-MS spectral data (in the positive ion mode) for the complexes **1**−**3** and **4** are listed in the Experimental Section. All these compounds display their respective molecular ion peak due to the $[M + H^+]$ ionic species ($[M - H_2O + H^+]$ for **3**). Unfortunately, we could not record the mass spectrum for **5** because of its lack of solubility in common organic solvents. In Figures 1a and 2a are displayed the isotope distribution pattern for the molecular ion peaks for two representative compounds **1** and **4**, respectively, together with their simulation patterns (Figures 1b and 2b). Similar results are also obtained for the rest of the compounds, thus providing support in favor of the

(19) Sheldrick, G. M. *Acta Crystallogr.* **1990**, *46A*, 467.
(20) Sheldrick, G. M. *SHELXL-97, Program for Crystal Structure Refinements*; University of Göttingen: Göttingen, Germany, 1996.
(21) *SAINT-plus, Software users guide*, Version 6.0; Bruker Analytical X-ray Systems: Madison, WI, 1999.
(22) Farrugia, L. J. *ORTEP-3* for WINDOWS; University of Glasgow: Glasgow, Scotland, 1997.
(23) (a) Bonadies, J. A.; Butler, W. M.; Pecoraro, V. L.; Carrano, C. J. *Inorg. Chem.* **1987**, *26*, 1218. (b) Oyaizu, K.; Dewi, E. L.; Tsuchida, E. *Inorg. Chem.* **2003**, *42*, 1070.
(24) (a) Dutta, S. K.; Samanta, S.; Mukhopadhyay, S.; Burckel, P.; Pinkerton, A. A.; Chaudhury, M. *Inorg. Chem.* **2002**, *41*, 2946. (b) Samanta, S.; Ghosh, D.; Mukhopadhyay, S.; Endo, A.; Weakley, T. J. R.; Chaudhury, M. *Inorg. Chem.* **2003**, *42*, 1508. (c) Samanta, S.; Mukhopadhyay, S.; Mandal, D.; Butcher, R. J.; Chaudhury, M. *Inorg. Chem.* **2003**, *42*, 6284.
(25) Fairhurst, S. A.; Hughes, D. L.; Leigh, G. J.; Sanders, J. R.; Weisner, J. *J. Chem. Soc., Dalton Trans.* **1994**, 2591.
(26) Nakamoto, K. *Infrared and Raman Spectra of Inorganic and Coordination Compounds*, 5th ed.; VCH-Wiley: New York, 1997.

Scheme 1[a]

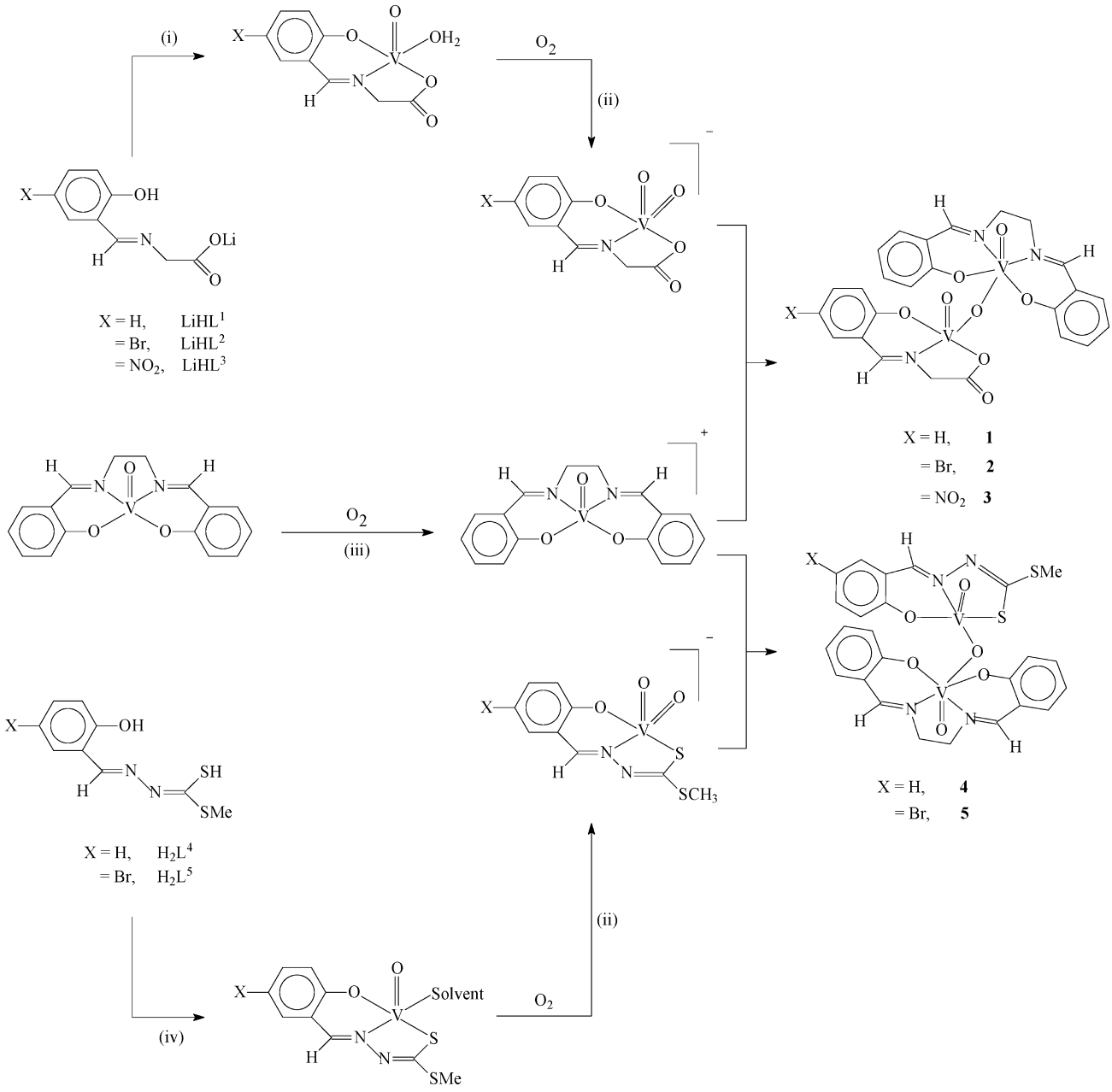

[a] Conditions: (i) $VOSO_4 \cdot 3H_2O$, ethanol, stir; (ii) cation-assisted aerial oxidation; (iii) anion-assisted aerial oxidation in CH_3CN; (iv) $VO(acac)_2$, CH_3CN, reflux.

proposed compositions involving the μ-oxo divanadium(V) core with coordination asymmetry.

Description of Crystal Structures. The molecular structures and the atomic labeling schemes for **2**, **3**, **4**, and **5** are shown in Figures 3, 4, 5, and Supporting Information, Figure S1, respectively, which provide a confirmatory evidence in support of their ligand asymmetric binuclear composition. Their selected metrical parameters are given in Tables 2 and 3. The asymmetric unit in each case comprises one neutral binuclear species excepting **3** and **5**, where an independent water and an acetonitrile molecule, respectively, are present in the asymmetric unit as solvent of crystallization. Complex **2** crystallizes in the triclinic space group $P\bar{1}$, and **3** in the monoclinic space group $P2_1/c$. There are two and four molecular weight units accommodated per unit cell, respectively, in the cases of **2** and **3**. The two halves of these molecules, bridged by an oxygen atom O(6), have different coordination geometry. In the case of **3**, the coordination environment around V(1) is distorted octahedral. Four donor atoms O(2), O(3), N(1), and N(2) from the Salen moiety occupy the basal plane and lie 0.0479, −0.0488, −0.0555, and 0.0563 Å (the corresponding values in the case of **2** are −0.0208, 0.0208, 0.0234, and −0.0234 Å), respectively, out of the least-squares plane through them. The apical positions are taken up by the terminal O(1) and the bridging O(6) oxygen atoms. The V(1) atom is marginally displaced by 0.2376 Å (0.2552 Å for **2**) from the least-squares basal plane toward the more tightly held terminal oxo-atom O(1). The

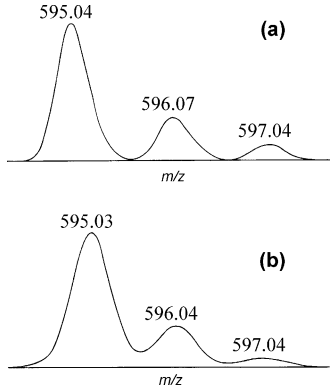

Figure 1. Molecular ion peak in the ESI mass spectrum (positive) for complex **1** in acetonitrile with (a) observed and (b) simulated isotopic distributions.

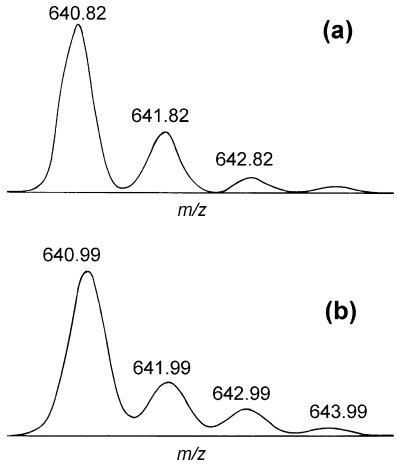

Figure 2. Molecular ion peak in the ESI mass spectrum (positive) for complex **4** in acetonitrile with (a) observed and (b) simulated isotopic distributions.

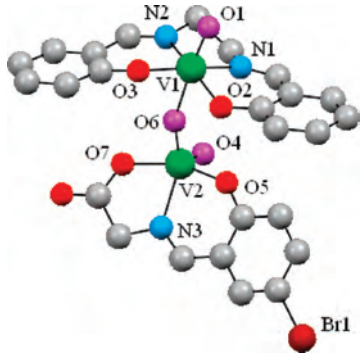

Figure 3. Molecular structure and atom-numbering scheme for **2**. Hydrogen atoms are omitted for clarity.

trans angles N(1)—V(1)—O(3) 160.29(8)° [159.18(7)°] and N(2)—V(1)—O(2) 156.68(7)° [157.71(7)°] are somewhat compressed and force the V(1) atom out of the respective basal planes. The distances and angles made by the donor atoms from the salen ligand (Table 2) are comparable with the corresponding values previously reported in compounds containing the $[V^{V}O(Salen)]^{+}$ unit.[23] On the other hand, the coordination geometry around V(2) is distorted square pyramidal. Three donor atoms O(5), N(3), and O(7) from the tridentate amino acid-based ONO ligands along with the

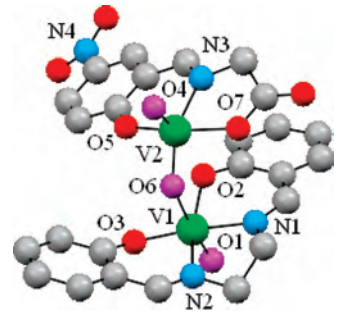

Figure 4. Molecular structure and atom-labeling scheme for **3.** Hydrogen atoms and the lattice water molecule have been omitted for clarity.

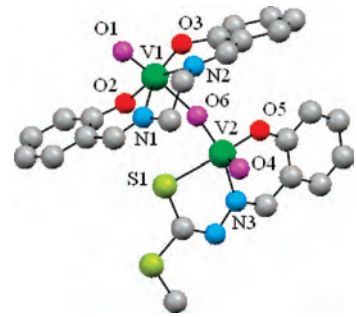

Figure 5. Perspective view (ball and stick) and atom-numbering scheme for **4.** Hydrogen atoms have been omitted for clarity.

bridging oxygen atom O(6) complete the equatorial plane around V(2) while the apical site is taken up by the terminal oxo-atom O(4). The deviations of O(5), N(3), O(7), and O(6) atoms from the least-squares basal plane are 0.0906, −0.0973, 0.0995, and −0.0928 Å (−0.1983, 0.2047, −0.2083, and 0.2019 Å), respectively. Here also the *trans* angles O(5)—V(2)—O(7) 153.93(7)° [155.60(7)°] and N(3)—V(2)—O(6) 146.96(7)° [135.42(7)°] are much short of linearity, giving indications of distortions in the meridian plane and account for the large displacement (0.4314 and 0.5013 Å in cases of **3** and **2**, respectively) of the V(2) atom out of the least-squares equatorial plane toward the apical oxo-atom O(4).

The perspective views of **4** and **5** resemble closely to those described above for **2** and **3**. Like **2**, the binuclear complexes **4** and **5** crystallize in the triclinic space group $P\bar{1}$ and have two molecular weight units accommodated in the unit cell. Like their predecessors, the molecules of **4** and **5** also have two halves with different coordination geometry. In the case of **4**, the coordination environment around V(1) is distorted octahedral and the four atoms O(2), O(3), N(1), and N(2) from the Salen moiety define the meridian plane and lie −0.0171, 0.0174, 0.0196, and −0.0199 Å (0.0445, −0.0439, −0.0515, and 0.0510 Å in the case of **5**), respectively, out of the least-squares plane through them. The V(1) atom is displaced by 0.2279 Å (0.2270 Å) out of the basal plane toward the apical oxygen atom O(1). The coordination environment around the second vanadium center V(2) is distorted square pyramidal in which the S(1), N(3), and O(5) donor atoms from the tridentate dithiocarbazate-based ONS ligands along with the bridging oxygen atom O(6) complete the equatorial plane. The apical position is taken up by the oxo- atom O(4). The *trans* angles S(1)—V(2)—O(5) 142.38(6)°

Table 2. Selected Bond Distances (Å) and Angles (deg) for the Complexes **2** and **3**

	2	**3**
	Bond Distances (Å)	
V(1)—O(1)	1.5903(16)	1.5940(17)
V(1)—O(2)	1.8255(15)	1.8705(15)
V(1)—O(3)	1.8228(15)	1.8140(16)
V(1)—N(1)	2.0828(17)	2.0864(19)
V(1)—N(2)	2.0979(18)	2.0836(19)
V(1)—O(6)	2.1772(15)	2.1658(16)
V(2)—O(4)	1.6130(17)	1.5994(16)
V(2)—O(5)	1.9062(15)	1.9223(16)
V(2)—O(6)	1.6504(15)	1.6848(15)
V(2)—O(7)	1.9488(16)	1.9636(16)
V(2)—N(3)	2.1472(17)	2.1454(18)
V(1)····V(2)	3.7633(5)	3.3084(6)
	Bond Angles (deg)	
O(1)—V(1)—O(2)	99.08(8)	96.61(8)
O(1)—V(1)—O(3)	102.61(8)	100.42(8)
O(1)—V(1)—N(1)	90.76(8)	90.95(8)
O(1)—V(1)—N(2)	95.70(8)	99.06(8)
O(1)—V(1)—O(6)	170.41(7)	174.67(8)
O(2)—V(1)—N(1)	86.18(7)	85.95(7)
N(1)—V(1)—N(2)	77.00(7)	76.65(8)
N(2)—V(1)—O(3)	85.75(7)	85.62(7)
O(3)—V(1)—O(2)	107.00(7)	108.42(7)
O(6)—V(1)—O(2)	83.34(6)	81.31(6)
O(6)—V(1)—N(1)	80.11(6)	84.02(7)
O(6)—V(1)—N(2)	79.48(6)	81.53(7)
O(6)—V(1)—O(3)	85.40(7)	84.91(7)
V(1)—O(6)—V(2)	158.76(9)	117.92(8)
O(4)—V(2)—O(5)	99.44(8)	99.59(8)
O(4)—V(2)—N(3)	114.59(8)	105.63(8)
O(4)—V(2)—O(7)	99.84(9)	100.75(8)
O(6)—V(2)—O(5)	94.19(7)	96.96(7)
O(6)—V(2)—N(3)	135.42(7)	146.96(7)
O(6)—V(2)—O(7)	93.20(8)	92.60(7)
O(2)—V(1)—N(2)	157.71(7)	156.68(7)
O(3)—V(1)—N(1)	159.18(7)	160.29(8)
O(5)—V(2)—O(7)	155.60(7)	153.93(7)
O(5)—V(2)—N(3)	82.29(6)	83.40(7)
N(3)—V(2)—O(7)	76.16(7)	75.53(7)
O(4)—V(2)—O(6)	109.84(9)	106.86(8)

Table 3. Selected Bond Distances (Å) and Angles (deg) for **4** and **5**

	4	**5**
	Bond Distances (Å)	
V(1)—O(1)	1.5923(17)	1.587(3)
V(1)—O(2)	1.8451(15)	1.816(3)
V(1)—O(3)	1.8146(16)	1.855(3)
V(1)—N(1)	2.0821(19)	2.081(3)
V(1)—N(2)	2.1007(19)	2.081(3)
V(1)—O(6)	2.1461(16)	2.140(3)
V(2)—O(6)	1.6713(16)	1.669(3)
V(2)—O(4)	1.6044(17)	1.596(3)
V(2)—O(5)	1.8892(16)	1.881(3)
V(2)—N(3)	2.1715(19)	2.178(3)
V(2)—S(1)	2.3662(7)	2.3694(13)
S(1)—C(24)	1.737(2)	1.717(4)
V(1)····V(2)	3.7921(7)	3.7395(13)
	Bond Angles (deg)	
O(1)—V(1)—O(2)	96.96(8)	100.78(15)
O(1)—V(1)—O(3)	101.68(9)	98.42(15)
O(1)—V(1)—N(1)	90.62(8)	96.12(15)
O(1)—V(1)—N(2)	96.03(8)	89.50(15)
O(1)—V(1)—O(6)	171.89(8)	173.28(14)
O(2)—V(1)—N(1)	86.80(7)	85.95(13)
N(1)—V(1)—N(2)	76.73(7)	76.23(13)
N(2)—V(1)—O(3)	84.99(7)	86.31(13)
O(2)—V(1)—O(3)	108.24(7)	108.40(13)
O(6)—V(1)—O(2)	84.22(7)	84.70(11)
O(6)—V(1)—N(1)	81.41(7)	80.29(12)
O(6)—V(1)—N(2)	80.69(7)	84.13(11)
O(6)—V(1)—O(3)	85.50(7)	83.36(12)
O(4)—V(2)—O(5)	110.51(8)	108.52(14)
O(4)—V(2)—N(3)	98.49(8)	97.58(14)
O(4)—V(2)—S(1)	103.54(7)	106.37(11)
O(4)—V(2)—O(6)	108.54(9)	108.10(14)
O(6)—V(2)—O(5)	96.96(7)	98.18(12)
O(6)—V(2)—N(3)	150.97(8)	152.72(13)
O(6)—V(2)—S(1)	86.72(6)	86.06(10)
V(1)—O(6)—V(2)	166.20(9)	157.79(16)
O(2)—V(1)—N(2)	159.08(7)	160.32(12)
O(3)—V(1)—N(1)	158.97(7)	157.13(14)
S(1)—V(2)—O(5)	142.38(6)	141.43(10)
S(1)—V(2)—N(3)	76.62(5)	77.83(9)
N(3)—V(2)—O(5)	82.91(7)	81.79(12)

[141.43(10)°] and N(3)—V(2)—O(6) 150.97(8)° [152.72(13)°] are also somewhat compressed, similar to **2** and **3**. The V(2) atom is appreciably displaced by 0.5377 Å (0.5308 Å) from the least-squares plane toward the terminal oxygen atom O(4).

Of particular interest in the structures of **2**−**5** are the conformations of the $V_2O_3^{4+}$ core which are susceptible to the steric requirements of the attached ligands as well as the coordination geometry of the participating vanadium centers.[4–9] In the present series of compounds, the angles at the vanadium centers subtended by the terminal and bridging oxo-atoms, that is, O(1)—V(1)—O(6) [170.41(7)−174.67(8)°] and O(4)—V(2)—O(6) [109.84(9)−106.86(8)°] are in the ranges, as expected for a nearly ideal octahedral and square pyramidal geometry around V(1) and V(2), respectively. The bridge angles V(1)—O(6)—V(2) for **2**, **4**, and **5** have values in the range 166.20(9)−157.79(16)°, in-between those expected for symmetric divanadium(V) compounds with octahedral (180°)[5] and square pyramidal (ca. 145°)[7,8a,b] vanadium centers. The V_2O_3 core in these compounds has a rare twist-angular structure,[9] a conformation somewhat intermediate between the regular *anti*-linear and *syn*-angular modes. An exception to this general trend in structure as observed in **2**, **4**, and **5** is, however, noticed in the structure of **3** where the V(1)—O(6)—V(2) bridge angle is 117.92(8)°, sufficiently lower than the values observed in rest of the compounds as described above. Also the basal planes around V(1) and V(2) in **3** are almost parallel as judged by the small

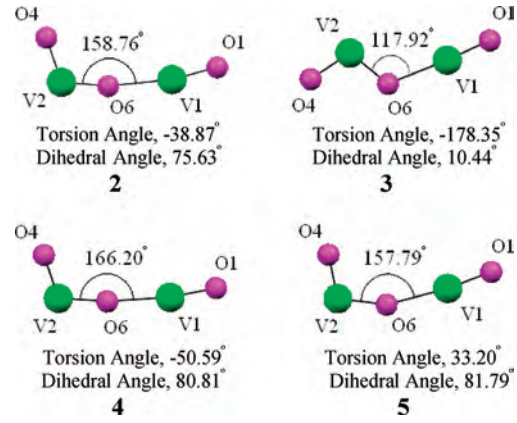

Figure 6. Relative orientations of the bridging [O(6)] and the terminal oxygen atoms [O(1) and O(4)] of the $V_2O_3^{4+}$ cores, found in **2**−**5**. The torsion angles represent the angles included within O(1)−V(1)···V(2)−O(4), and the dihedral angles indicate the angles between the least-squares equatorial planes surrounding the vanadium centers V(1) and V(2).

Table 4. ^{1}H NMR Spectral Data (δ, ppm)[a] for the Complexes **1**−**3** in DMSO-d_6 at 293 K

1		2		3		assignments
9.37 s	2H	9.39 s	2H	9.35 s	2H	H(7), H(7′)
8.68 s	1H	8.66 s	1H	8.88 s	1H	H(15)
7.99 (7.35) d	2H	8.11−7.70 m	4H	7.98 (7.56) d	2H	H(5), H(5′)
7.83 (7.39) t	2H			7.83 (7.57) t	2H	H(4), H(4′)
7.44 (7.65) d	1H	7.63 s	1H	8.51 (2.88) d	1H	H(13)
7.37 (7.62) t	1H	7.45(8.07) d	1H	8.18 (2.59) dd	1H	H(11)
7.26 (7.36) t	2H	7.16 brs	2H	7.27 (7.41) t	2H	H(3), H(3′)
7.14 (8.13) d	2H	6.98(7.99) d	2H	7.14 (8.22) d	2H	H(2), H(2′)
6.76−6.69 m	2H	6.68(8.31) d	1H	6.85 (9.30) d	1H	H(10), H(12)[b]
4.49 s	2H	4.50 s	2H	4.60 s	2H	H(16)
4.45, 4.22 (6.57) q	4H	4.20 brs	4H	4.44, 4.19 (6.42) q	4H	H(8), H(8′)

[a] Chemical shifts (δ) relative to internal TMS. Proton labels are as in the inset in Figure 7. s, singlet; d, doublet; t, triplet; dd, double−doublet; brs, broad singlet; q, AB quartet. Values in the parentheses represent coupling constants (J in Hz). [b] H(12) proton is absent in **2** and **3**.

Table 5. ^{1}H NMR Spectral Data (δ, ppm)[a] for the Complexes **4** and **5** in DMSO-d_6 at 293 K

4		5		assignments
9.35 s	2H	9.36 s	2H	H(7), H(7′)
8.98 s	1H	9.00 s	1H	H(15)
7.97 (6.82) d	2H	7.98 (7.31) d	2H	H(5), H(5′)
7.81 (6.94) t	2H	7.84 (7.54) t	2H	H(4), H(4′)
7.61 (7.58) d	1H	7.85 s	1H	H(13)
7.38 (7.59) t	1H	7.48 (2.55) dd	1H	H(11)
7.25 (6.91) t	2H	7.28 (7.18) t	2H	H(3), H(3′)
7.13 (7.81) d	2H	7.16 (8.10) d	2H	H(2), H(2′)
6.86−6.77 m	2H	6.76 (8.86) d	1H	H(12)[b], H(10)
4.42, 4.21 (5.63) q	4H	4.43, 4.20 (5.89) q	4H	H(8), H(8′)
2.49 s	3H	2.52 s	3H	H(17)

[a] Chemical shifts (δ) relative to internal TMS. Proton labels are as in the inset in Figure 8. s, singlet; d, doublet; t, triplet; dd, double−doublet; q, AB quartet. Values in the parentheses represent the coupling constants (J in Hz). [b] H(12) proton is absent in **5**.

dihedral angle (10.44°) between them while in the rest of the compounds, the concerned planes are nearly orthogonal with dihedral angles 75.63°, 80.81°, and 81.79° for **2**, **4**, and **5**, respectively. A clear manifestation of these differences in structural parameters is evident from the torsion angle O(1)−V(1)····V(2)−O(4) (Figure 6), which is −178.35° for **3**, much larger than the values −38.87°, −50.59°, and 33.20° observed in the rest of the compounds. All these have led us to conclude that the $V_2O_3^{4+}$ core in **3** is different from the rest of the molecules in this series and has an *anti*-angular structure as displayed in Figure 6.

Another important structural feature of these compounds that deserves mention is the *trans* location of the bridging oxygen atom O(6) relative to the terminal oxo-atom O(1) attached to the octahedral vanadium center V(1). Such a *trans* arrangement is unique in divanadium compounds containing $V_2O_3^{n+}$ core.[4–9] In consequence, the V(1)−O(6) distances [2.140(3)−2.1772(15) Å] in these compounds are significantly enlarged because of the *trans* labilizing influence of the terminal oxo-atom O(1), compared with the other bridging distances V(2)−O(6) [1.6504−1.6548 Å]. In effect, the enlarged V(1)····V(2) separations in **2**−**5** [3.7921(7)−3.3084(6) Å] are by far the largest among their peers (divanadium compounds containing a V_2O_3 core) reported thus far in the literature.[4–9]

Crystal structures of a few mononuclear salen-based vanadium(V) complexes, that is, [VO(Salen)A] (A = ClO_4^-, BF_4^-)[23] and [VO(Salen)B]$^+$ (B = CH_3CN, MeOH, DMSO, and H_2O)[23,27–29] have been reported in recent times. These compounds have closely comparable structures with almost straight O_t−V−D (D is the *trans* donor atom) angles [174.82(19)−172.5(2)°] and much elongated V−D distances [2.508(7)−2.282(4) Å] because of the labilizing influence of the terminal oxo- atom as observed in **1**−**5**.

^{1}H NMR Spectroscopy. ^{1}H NMR spectra of **1**−**5** have been measured at room temperature in DMSO-d_6, and the data are summarized in Tables 4 and 5. The lithium salt of the amino acid-based ligands ($LiHL^1$−$LiHL^3$) display a broad resonance in the same solvent at 14.2 ppm because of the phenolic-OH proton. The corresponding signal appears at 10.1 ppm in the remaining two tridentate ligands (H_2L^4 and H_2L^5) along with a broad peak at 11.1 ppm due to the SH proton. All these signals due to the acidic protons along with the phenolic-OH protons of the Salen moiety (appears at 13.3 ppm) are missing in the complexes **1**−**5**.

The spectral profiles of **1** and **5** are displayed in Figures 7 and 8, respectively, as representatives for each type of complexes along with their possible interpretations. Spectrum of **1** contains a pair of singlets at 9.37 and 8.68 ppm (in 2:1 intensity ratio), corresponding to the presence of two different types of azomethine moieties in the molecule. Corresponding signals in **5** appear at 9.36 and 9.00 ppm, respectively. All the aromatic protons in **1** appear in the 8.0−6.5 ppm region (8.0−6.75 ppm range in **5**) with expected splitting patterns. Of particular interest here is the triplet appearing at 7.37 ppm (J = 7.62 Hz) due to the H(11) proton in the spectrum of **1**. Substitution of nitro- and bromine at C(12) in **3** and **5**, respectively, make the same H(11) proton to appear (Figure 8, inset) as a pair of doublets at 7.50 and 7.47 ppm (8.20 and 8.17 ppm for **3**) due to *ortho-meta* coupling. Observance of small J values of 2.59 and 2.55 Hz for **3** and **5**, respectively, provides an indication for such weak couplings. The ethylenic protons H(8) and H(8′) are diastereotopic in these complexes because of the rigidity of the metal-bound bridge-head moiety in the coordinated salen part and appear as an AB spin system with δ_A = 4.45 and δ_B = 4.22 ppm (J_{AB} = 6.57 Hz) in **1**. A sharp singlet at 4.49 ppm is characteristic of the H(16) protons of the amino acid part in

(27) Choudhary, N. F.; Hitchcock, P. B.; Leigh, G. J. *Inorg. Chim. Acta* **2000**, *310*, 10.
(28) MacLachlan, M. J.; Park, M. K.; Thompson, L. K. *Inorg. Chem.* **1996**, *35*, 5492.
(29) Banci, L.; Bencini, A.; Dei, A.; Gatteschi, D. *Inorg. Chim. Acta* **1984**, *84*, L11.

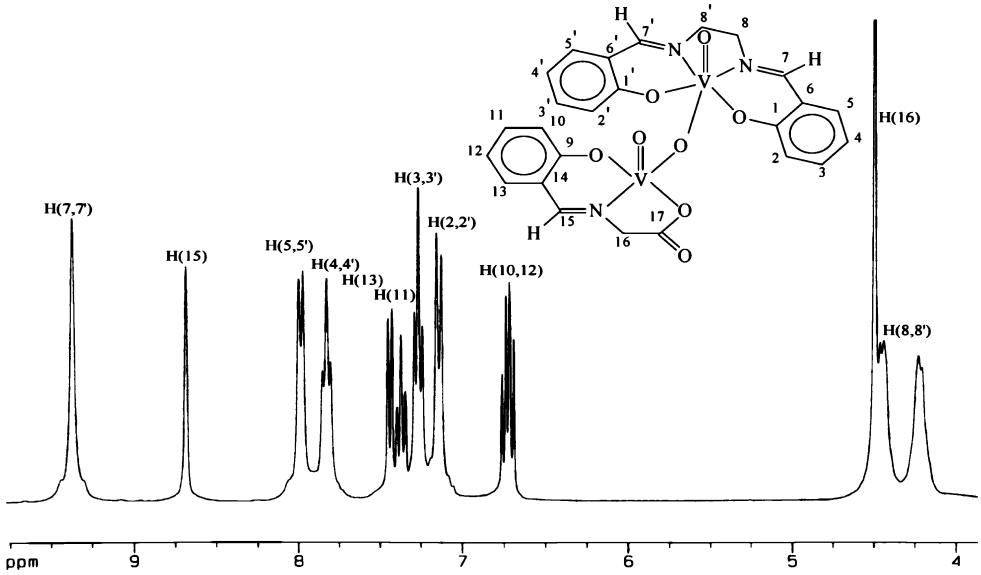

Figure 7. ^{1}H NMR spectrum of compound **1** in DMSO-d_6 at 293 K.

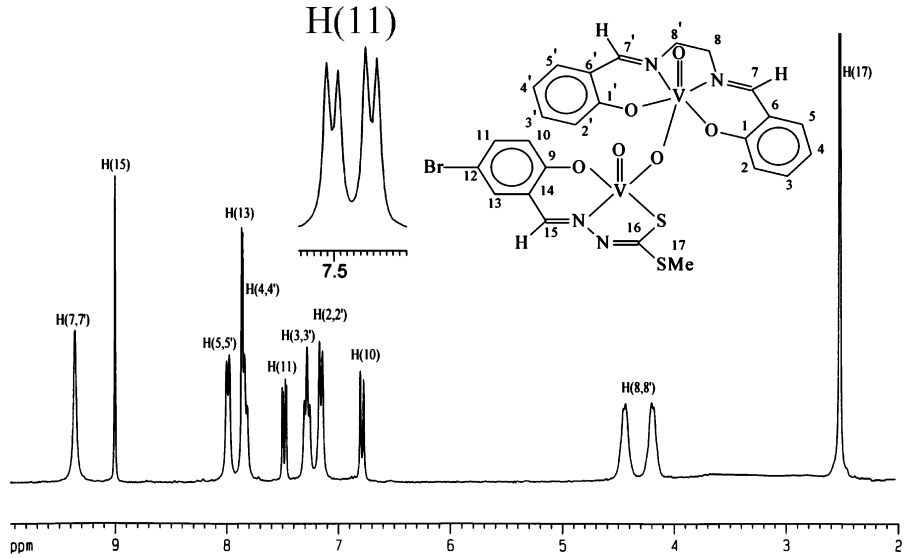

Figure 8. ^{1}H NMR spectrum of compound **5** in DMSO-d_6 at 293 K. The inset shows the appearance of the H(11) proton as a pair of doublets due to *ortho-meta* coupling.

1. All these and the remaining signals along with their observed splitting patterns are in conformity with the presence of asymmetric ligand environments around the vanadium centers in **1**−**5** as exist in solution.

^{51}V NMR Spectroscopy. To understand more about the solution structures of **1**−**5**, ^{51}V NMR spectra of these complexes have been measured in DMSO-d_6 solution at room temperature. Results are displayed in the Experimental Section. Almost identical features are obtained in all the cases. Spectra for **1** and **5** are displayed in Figure 9a,b as representative for each type of complexes. Two sharp signals are obtained in each case, both in the negative region of the chemical shift. In the the case of **1**, a very sharp peak (peak I), appears at −533 ppm which is more likely due to a [V^VOL^1] moiety[7b] while the other peak, moderately sharp in appearance (peak II), shows up at −574 ppm arises from the [V^VO(Salen)] part of the compound.[25,27] Corresponding signals in the spectrum of **5** appear at −466 and −574 ppm, respectively.

Thus, a change in the donor atoms set from ONS to ONO type in the tridentate ligand around the square pyramidal vanadium(V) center generates a remarkable upfield shift (by ca. 70 ppm) of the corresponding ^{51}V NMR signal. However, as expected, the signals due to the [V^VO(Salen)] moiety remain unchanged at −574 ppm in both compounds. The results again are in compliance with the asymmetry in ligand environments around the vanadium centers in **1**−**5** when present in solution.

Electronic Spectroscopy. Electronic absorption spectra of the complexes **1**−**5** in DMSO are also summarized in the Experimental Section. The spectra in general are featureless, involving a lone LMCT band [$PhO^- \rightarrow V(d\pi)$] at about 575 nm. All the remaining bands appearing in the UV regions are due to the ligand internal transitions.

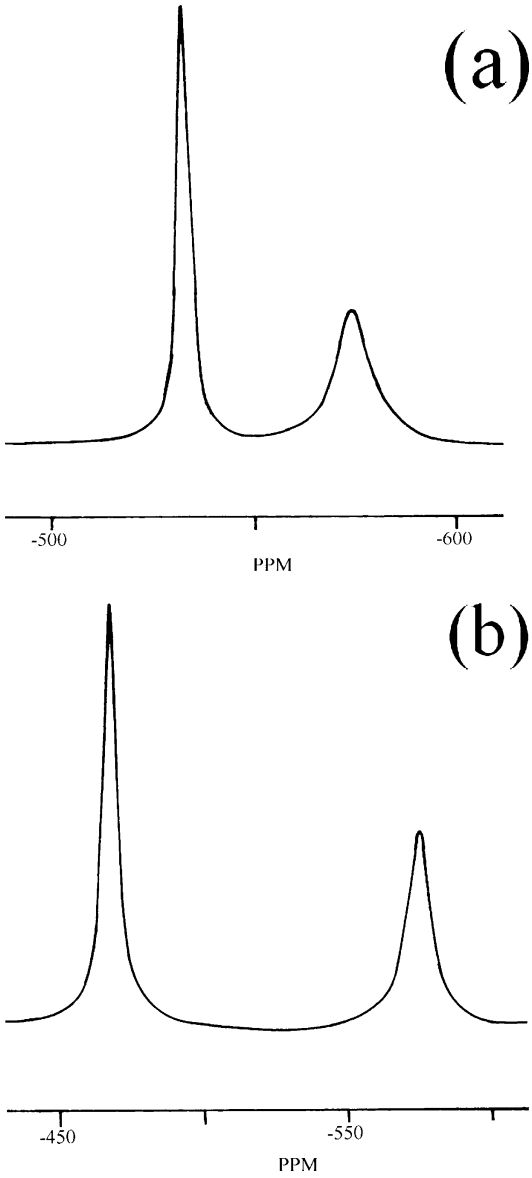

Figure 9. ^{51}V NMR spectra of the complexes (a) **1** and (b) **5** in DMSO-d_6 solution at room temperature showing retention of binuclear structures in solution.

Electrochemistry. The redox behavior of **1**−**5** have been examined by CV at a platinum working electrode under an envelope of purified dinitrogen in DMSO solution (0.1 M TBAP) at room temperature in the potential window of −2.0 to +2.0 V versus Ag/AgCl reference. The ligands are electrode inactive in this potential range. Voltammetric features of **1** and **4**, each representing a typical group of compounds, are displayed in Figures 10 and 11, respectively. The data obtained are summarized in Table 6. The voltammogram of **1** includes a couple of reduction processes which include a reversible process at $(E_{1/2})_I = 0.45$ V (process A) and an irreversible process at $E_{pc} = -1.48$ V (process B). In addition to the processes A and B, the voltammogram of **4** also includes a third redox process (process C) at $(E_{1/2})_{II} = -1.74$ V. All these processes are cathodic as indicated by steady-state voltammetry (using an ultramicroelectrode, 10 μM diameter) and involve an identical number of electron(s), established by normal pulse voltammetry (NPV),

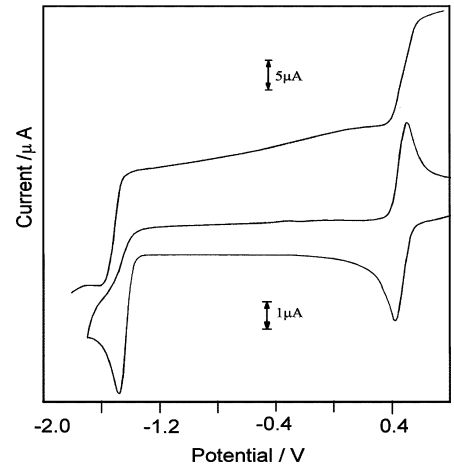

Figure 10. Cyclic and normal pulse voltammograms of **1** in DMSO (0.1 M TBAP) at room temperature using a platinum-disk working electrode; scan rate 100 mVs^{-1} and potentials vs Ag/AgCl.

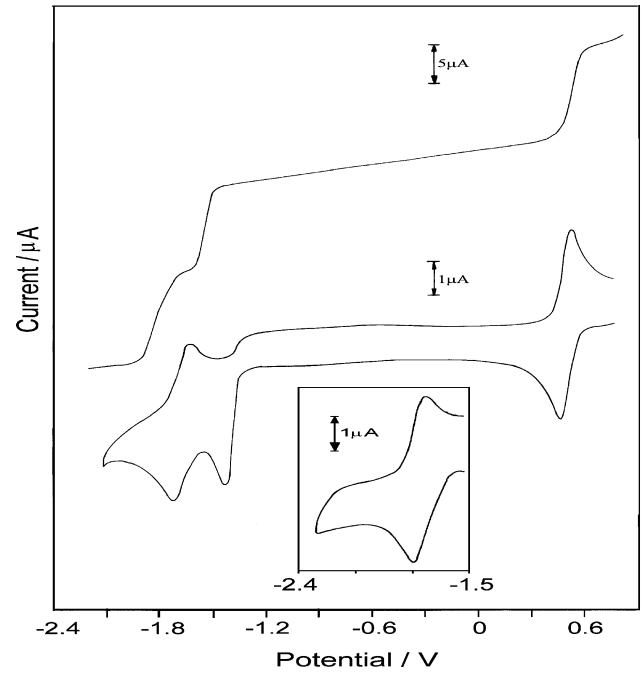

Figure 11. Cyclic and normal pulse voltammograms of **4** in DMSO; potentials vs Ag/AgCl, 0.1 M TBAP at a platinum working electrode, scan rate 100 mVs^{-1}. The inset shows a lone quasireversible process for the mononuclear vanadium(V) compound [L^4VO(OCH$_3$)] at an identical experimental condition.

also shown in Figures 10 and 11. On the basis of comparison with the ferrocenium/ferrocene couple (ΔE_p, 70 mV; $i_{pc}/i_{pa} = 1$ at 100 mV s^{-1}), process A may be appropriately described as reversible (ΔE_p, 69 mV; $i_{pc}/i_{pa} = 0.99$ at 100 mV s^{-1}) while process C (in the case of **4**) may be labeled as a quasireversible (ΔE_p, 110 mV) in the electrochemical sense.[30]

Electrochemical behavior of [VO(Salen)] is well documented in the literature.[31] Taking a cue from these studies, one can consider processes A and B in **1** to be restricted on the [VO(Salen)] part of the complex. While process A is believed to originate from a [VO(Salen)]$^{1+/0}$ couple, process B on the other hand is due to a [V(Salen)]$^{2+/1+}$ electron-

Table 6. Summary of Electrochemical Data[a]

	process A				process B	process C	
compound	$(E_{1/2})_{II}$/V[b]	ΔE_p/mV[c]	i_{pc}/i_{pa}	n	E_{pc}/V	$(E_{1/2})_{II}$/V[b]	ΔE_p/mV[c]
1	0.45	73	1.00	0.98 ± 0.05	−1.48		
2	0.44	62	0.90		−1.49		
3	0.42	66	0.99		−1.52		
4	0.42	69	0.99	1 ± 0.1	−1.50	−1.74	110
5	0.43	71	0.99		−1.55	−1.83	125

[a] All potentials vs Ag/AgCl reference. [b] $E_{1/2} = 0.5\ (E_{pc} + E_{pa})$, calculated from CV data. [c] $\Delta E_p = E_{pa} \sim E_{pc}$ at a scan rate of 100 mV s^{-1}.

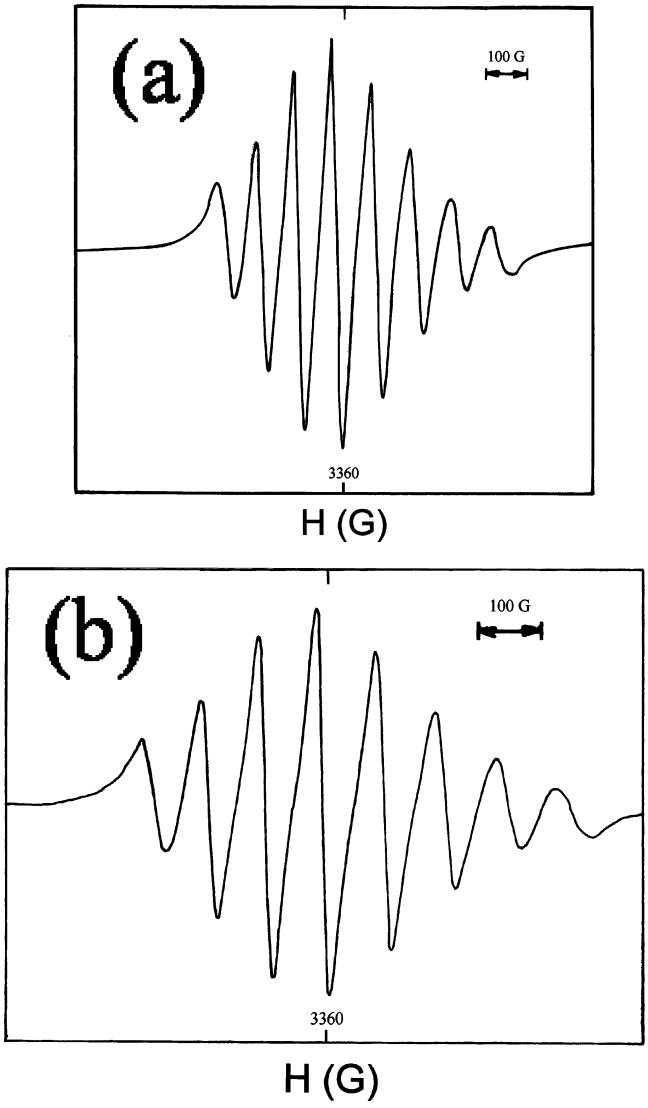

Figure 12. The X-band EPR spectra at room temperature of the catholyte solutions (in DMSO), generated electrochemically by coulometric reduction of compounds (a) **1** and (b) **5** (E_w set at 0.2 V vs Ag/AgCl).

transfer involving a putative nonoxo vanadium species. The electrochemical results thus indicate the involvement of a mixed-oxidation species in process A as shown by equation 1.

$$[L^1OV^V(\mu\text{-}O)V^VO(Salen)]^0 \underset{(E_{1/2})_t}{\overset{\text{Process A}\ +e^-}{\rightleftharpoons}} [L^1OV^V(\mu\text{-}O)V^{IV}O(Salen)]^{1-} \quad (1)$$

This mixed-oxidation species is sufficiently stable in solution as indicated by the steady-state voltammograms recorded before and after the electrolysis of **1** (Supporting Information, Figure S2). However, at a much negative potential, somewhere before −1.5 V, this mixed oxidation species possibly goes through a process of decomposition to generate two or more products, including $[V^{IV}O(Salen)]$ which undergoes an irreversible reduction at −1.5 V (process B), tentatively with the elimination of a terminal oxygen atom from the vanadium coordination sphere.[31c] The remaining part $[L^1V^vO]$ involving the amino acid-based tridentate ligand remains electrode inactive through out the potential range of this study.

The quasireversible process observed at −1.74 V (process C) for **4** appears to involve the reduction of $[L^4V^VO]$ part of $[\mathbf{4}]^-$, obtained during the decomposition. To understand more about this process, a control CV experiment has been carried out under identical experimental conditions using a closely similar mononuclear vanadium(V) compound $[L^4VO(OCH_3)]$.[7a] The voltammogram is displayed in Figure 11 (inset) that involves a lone quasireversible process (ΔE_p, 95 mV; $i_{pc}/i_{pa} = 0.97$) at $E_{1/2} = -1.74$ V due to a vanadium-centered $[L^4VO(OCH_3)]^{0/1-}$ reduction. The close similarity of this voltammogram with process C in **4** provides convincing evidence in favor of process C being a vanadium centered electron-transfer involving the $[L^4V^vO]$ part of compound **4**.

Electron stoichiometry for process A of both **1** and **4** has been confirmed further by constant potential coulometric experiments with a platinum-gauze working electrode, done at a potential past the reduction process (E_w set at 0.2 V vs Ag/AgCl). Results ($n = 0.98 \pm 0.05$ for **1** and 1 ± 0.1 for **4**) are in conformity with the single-electron stoichiometry for this process as shown by equation 1. Similar experiments for the remaining processes (B and C) did not yield any meaningful results because of an unidentified electrode reaction(s).

EPR Spectroscopy. EPR spectra of the catholyte solutions obtained after coulometric reduction of **1** and **5** have been recorded at room temperature and are displayed in Figure 12. The spectra in both cases feature an 8-line profile (^{51}V, $I = 7/2$) with $\langle g \rangle = 1.991$ and $\langle A \rangle = 89 \times 10^{-4}$ cm^{-1} for **1**. Corresponding values are 1.990 and 88×10^{-4} cm^{-1} for **5**. Of particular interest are the observed $\langle A \rangle$ values here which are twice as much as that of a typical 15-line spectrum, displayed by a delocalized mixed-oxidation divanadium (IV/

(30) Brown, E. R.; Large, R. F. Electrochemical Methods. In *Physical Methods in Chemistry*; Weissberger, A., Rossiter, B. Eds.; Wiley-Interscience: New York, 1971; Part IIA, Chapter VI.
(31) (a) Kapturkiewicz, A. *Inorg. Chim. Acta* **1981**, *53*, L77. (b) Seangprasertkij, R.; Riechel, T. L. *Inorg. Chem.* **1986**, *25*, 3121. (c) Tsuchida, E.; Yamamoto, K.; Oyaizu, K.; Iwasaki, N.; Anson, F. C. *Inorg. Chem.* **1994**, *33*, 1056; and references therein.

V) compound containing a V_2O_3 core[7] because of the reasons already reported by Slichter.[32] Thus, in the absence of a mononuclear vanadium(IV) species in solution, the observed $\langle A \rangle$ values for the catholyte solutions of **1**−**5** provide clear evidence of the trapped-valence nature of the reduced mixed-oxidation binuclear species $[\mathbf{1}-\mathbf{5}]^{1-}$ in the time-scale of EPR spectroscopy.[4c] The unpaired electron is therefore localized on one of the vanadium centers, preferably on the [VO(Salen)] part, indicating class A character, according to the Robin−Day classification of mixed-valence compounds.[33]

Electronic spectra of the catholyte solutions failed to provide any band in the NIR region, expected for a possible intervalence charge-transfer in the mixed-oxidation product, thus lending support to the results of EPR spectroscopy in confirming the trapped-valence nature of the reduced divanadium(IV/V) product.

Concluding Remarks

Isovalent μ-oxo divanadium(V) compounds [$LOV^V(\mu$-$O)V^VO$(Salen)] (**1**−**5**) with ligands providing the donor set and coordination number asymmetry in tandem have been synthesized. In a typical compound, one of the vanadium centers has an octahedral geometry, completed by the tetradentate Salen ligand. The second metal center has a square pyramidal geometry made up with a tridentate biprotic Schiff-base ligand based on either the amino acid part (**1**−**3**) or the dithiocarbazate (**4**, **5**). All these compounds, save **3**, have closely similar structures (triclinic space group, $P\bar{1}$) with a rare type of *twist*-angular V_2O_3 core.[9] Crystals of **3** on the other hand have a monoclinic space group ($P2_1/c$) with an *anti*-angular V_2O_3 core structure.[7b] The V(1)···V(2) separations are unprecedentedly larger in these compounds compared to their peers (compound with a V_2O_3 core) reported thus far in the literature.[4−9] The angularity in the structure of this V_2O_3 core probably remains intact even in solution and blocks all sorts of electronic communications between the participating vanadium centers as revealed from the ^{51}V NMR, CV, and EPR studies. The valence-trapped situation in the one-electron reduced products $[\mathbf{1}-\mathbf{5}]^{1-}$ probably arises from the bent V−O−V bridge [166.20(9)−117.92(8)°], preventing the symmetry constrained vanadium d_{xy} orbitals, containing the unpaired electron, to overlap effectively via the pπ orbital of the bridging oxygen atom.[34]

Acknowledgment. This work was supported by the Council of Scientific and Industrial Research (CSIR), New Delhi. Three of us (P.B.C., S.B., and A.A.) also thank the CSIR for the award of Research Fellowships. M.C. thanks the authorities of Sophia University, Japan for a Lecturing-Research Grant, 2006.

Supporting Information Available: ORTEP diagram of **5**, the steady-state voltammograms of **1** (Figure S1 and S2, PDF) and the X-ray crystallographic files in CIF format for the compounds **2**, **3**, **4**, and **5**. This material is available free of charge via the Internet at http://pubs.acs.org.

IC800208W

(32) Slichter, C. P. *Phys. Rev.* **1955**, *99*, 478.
(33) Robin, M. B.; Day, P. *Adv. Inorg. Chem. Radiochem.* **1967**, *10*, 247.
(34) Young, C. G. *Coord. Chem. Rev.* **1989**, *96*, 89.